AFOSR-TR- 86-0010

(2)

# FINAL TECHNICAL REPORT

February 1 1984 - July 31, 1985

| | |
|---|---|
| ARPA Order Number: | 4944 |
| Program Code: | 4D60 |
| Name of Contractor: | The Trustees of Columbia University in the City of New York |
| Effective Date of Contract: | February 1, 1984 |
| Contract Expiration Date: | July 31, 1985 |
| Amount of Contract: | $86,387 |
| Contract Number: | F49 620-84-C-0019 |
| Principal Investigator: | C. H. Scholz<br>914-359-2900 |
| Program Manager & Phone No.: | Mr. Henry R. Radoski<br>(202) 767-4904 |
| Short Title of Work: | Quasi-static experiments designed to explain strength of rock in an Explosion |



Sponsored by
Advanced Research Projects Agency
ARPA Order No. 4944
Monitored Under Contract #F49620-84-C-0019



Lamont-Doherty Geological Observatory of Columbia University
Palisades, New York 10964

November 1985

Unclassified
SECURITY CLASSIFICATION OF THIS PAGE

# REPORT DOCUMENTATION PAGE

| | |
|---|---|
| 1a. REPORT SECURITY CLASSIFICATION: Unclassified | 1b. RESTRICTIVE MARKINGS |
| 2a. SECURITY CLASSIFICATION AUTHORITY | 3. DISTRIBUTION/AVAILABILITY OF REPORT: Approved for Public Release Distribution Unlimited |
| 2b. DECLASSIFICATION/DOWNGRADING SCHEDULE | |
| 4. PERFORMING ORGANIZATION REPORT NUMBER(S) | 5. MONITORING ORGANIZATION REPORT NUMBER(S): AFOSR-TR-86-0010 |
| 6a. NAME OF PERFORMING ORGANIZATION: Lamont-Doherty Geological Obs. of Columbia University; 6b. OFFICE SYMBOL (If applicable) | 7a. NAME OF MONITORING ORGANIZATION: Air Force Office of Scientific Research |
| 6c. ADDRESS (City, State and ZIP Code): Palisades, New York 10964 | 7b. ADDRESS (City, State and ZIP Code): Directorate of Physical & Geophysical Sciences Bolling AFB, DC 20332 - 6448 |
| 8a. NAME OF FUNDING/SPONSORING ORGANIZATION: Air Force Office of Scientific Research; 8b. OFFICE SYMBOL (If applicable): NP | 9. PROCUREMENT INSTRUMENT IDENTIFICATION NUMBER: F49620-84-C-0019 |
| 8c. ADDRESS (City, State and ZIP Code): Building 410 Bolling AFB, DC 20332 - 6448 | 10. SOURCE OF FUNDING NOS. |

| PROGRAM NO. | PROJECT NO. | TASK NO. | WORK UNIT NO. |
|---|---|---|---|
| 61102F | 2309 | A1 | N/A |

11. TITLE (Include Security Classification): "Quasi-static experiments designed to explain strength of rock in an explosion"

12. PERSONAL AUTHOR(S): Christopher H. Scholz

| 13a. TYPE OF REPORT | 13b. TIME COVERED | 14. DATE OF REPORT (Yr., Mo., Day) | 15. PAGE COUNT |
|---|---|---|---|
| Final | FROM 2/1/84 TO 7/31/85 | November 1985 | 31 |

16. SUPPLEMENTARY NOTATION: ---

| 17 COSATI CODES | | |
|---|---|---|
| FIELD | GROUP | SUB. GR. |
| | | |
| | | |

18. SUBJECT TERMS (Continue on reverse if necessary and identify by block number)

19. ABSTRACT (Continue on reverse if necessary and identify by block number)

The Bridgman ring experiment, in which a hard rubber ring slipped over a steel rod was observed to split when subjected to a hydrostatic confining pressure, was repeated using pyrex glass rings. Three cases were studied; 1) in which both ring and rod were unjacketed, 2) in which the inner wall of the ring was sealed from the pressure medium, and, 3) in which both the rod and ring were completely jacketed. In the first two cases, the ring was observed to split abruptly, with a single axial crack when confining pressure reached a critical level. In the third case no abrupt failure occurred but a number of axial cracks were found to have formed, grown stably, but not penetrate the outer wall of the ring. The first two cases are explained by hydraulic fracturing of the ring. Observations and analysis indicate that in the third case the cracks initiated at flaws on the inner surface of the ring and propagated outwards in a stable manner. This case, in which a tensile crack propagates in an all around compressive stress field, provides some insight into axial cracking of rock in triaxial compression and tensile failure of rock under radial shock loading.

| 20. DISTRIBUTION/AVAILABILITY OF ABSTRACT | 21. ABSTRACT SECURITY CLASSIFICATION |
|---|---|
| UNCLASSIFIED/UNLIMITED ☒ SAME AS RPT. ☒ DTIC USERS ☐ | Unclassified |

| 22a. NAME OF RESPONSIBLE INDIVIDUAL | 22b. TELEPHONE NUMBER (Include Area Code) | 22c. OFFICE SYMBOL |
|---|---|---|
| Ralph E. Kelley | (202) 767-4908 | NP |

DD FORM 1473, 83 APR — EDITION OF 1 JAN 73 IS OBSOLETE.

UNCLASSIFIED
SECURITY CLASSIFICATION OF THIS PAGE

**PROJECT SUMMARY**

In the failure of rock in an underground nuclear explosion it has often been assumed that failure occurs in compression, and this has led to some difficulties in modeling. In conventional blasting applications, however, it has sometimes been assumed that failure near the borehole is in tension, although the reason for this has remained unexplained. This type of paradox, in which a material was observed to fail in tension under an overall compressive stress field, was discussed long ago by P.W. Bridgman, who failed to explain it. A further examination of this phenomenon was undertaken to see if it might shed light on this problem.

The Bridgman ring experiment, in which a hard rubber ring slipped over a steel rod was observed to split when subjected to a hydrostatic confining pressure, was repeated using pyrex glass rings. Three cases were studied: 1) in which both ring and rod were unjacketed, 2) in which the inner wall of the ring was sealed from the pressure medium, and, 3) in which both rod and ring were completely jacketed. In the first two cases, the ring was observed to split abruptly, with a single axial crack when confining pressure reached a critical level. In the third case no abrupt failure occurred but a number of axial cracks were found to have formed, grown stably, but not penetrate the outer wall of the ring. The first two cases are explained by hydraulic fracturing of the ring. Observations and analysis indicate that in the third case the cracks initiated at flaws on the inner surface of the ring and propagated outwards in a stable manner. This case, in which a tensile crack propagates in an all around compressive stress field, provides some insight

(cont)

into axial cracking of rock in triaxial compression and tensile failure of rock under radial shock loading.

These results are suggestive but not conclusive as regards the seismic coupling problem. They should be considered in future experimental and numerical modelling studies of this phenomenon.

Our research and conclusions are summarized in the attached paper by C. H. Scholz, G. Boitnott and S. Nemat-Nasser.



B

FINAL TECHNICAL REPORT

# Quasi-static Experiments Designed to Explain the Strength of Rock in an Explosion

C. H. Scholz

Contract F49620-84-C-0019

Quasi-Static Experiments Designed to
Explain Strength of Rock in an Explosion

# THE BRIDGMAN RING PARADOX REVISITED

TABLE OF CONTENTS

# The Bridgman Ring Paradox Revisited

C.H. Scholz, G. Boitnott

Lamont-Doherty Geological Observatory and

Department of Geological Sciences of Columbia University

Palisades, NY 10964

and

S. Nemat-Nasser

Dept. of Applied Mechanics and Engineering Sciences, Univ. of

Calif., San Diego

La Jolla, California

## Abstract

The Bridgman ring experiment, in which a hard rubber ring slipped over a steel rod was observed to split when subjected to a hydrostatic confining pressure, was repeated using pyrex glass rings. Three cases were studied; 1) in which both ring and rod were unjacketed, 2) in which the inner wall of the ring was sealed from the pressure medium and, 3) in which both rod and ring were completely jacketed. In the first two cases, the ring was observed to split abruptly, with a single axial crack when confining pressure reached a critical level. In the third case no abrupt failure occurred but a number of axial cracks were found to have formed, grown stably, but not penetrate the outer wall of the ring. The first two cases are explained by hydraulic fracturing of the ring. Observations and analysis indicate that in the third case the cracks initiated at flaws on the inner surface of the ring and propagated out-

wards in a stable manner. This case, in which a tensile crack propagates in an all around compressive stress field, provides some insight into axial cracking of rock in triaxial compression and tensile failure of rock under radial shock loading.

## Introduction

Under static and dynamic equilibrium, stress or strain failure criteria are generally considered equivalent. Bridgman [1] discussed a number of modes of failure peculiar to high pressures. By describing two phenomena that were paradoxical to him, Bridgman concluded (pp. 91-93): "For myself, I am exceedingly sceptical as to whether there is any such thing as a genuine criterion of rupture". These two phenomena are called 'the pinching-off effect' and the 'ring paradox'. In this paper we briefly review the pinching-off effect and compare those results with our results in repeating the ring paradox experiment. These results, in which we attempt to satisfactorily explain the paradox, provide some insight into axial splitting in triaxial testing, and a case of dynamic rock failure, vis., failure from shock loading due to an explosion within a cylindrical or spherical cavity.

The Pinching-off Effect. This experiment, shown in Fig. 1a, consists of a rod, unsupported at either end, which is inserted through seals into a pressure vessel and subjected to fluid confining pressure. With ductile materials, necking was observed and the rod pinched-off in a manner typical of rupture in tension. When brittle rods were used they failed with a fracture perpendicular to the rod axis, often somewhat near the middle of the rod, and were explosively discharged from the ends of pressure vessel.

In this latter case Bridgman argued that since failure did not occur near the seals where a stress concentration might exist, and since it could be shown that there was no stress in the axial direction in the rod, that a stress fracture criteria could not explain the failure of the rod. At best only a strain criteria could be used, since there was an extensional strain in the axial direction.

Jaeger and Cook [2] repeated these experiments with rock. They showed that failure occurred when the confining pressure was approximately equal to the tensile strength of the rock and was due to fluid intrusion into the rock, thus producing a tensile effective stress in the rod sufficient for fracture.

However, Jaeger and Cook [2] also performed the same experiments with specimens jacketed with various materials. In that case they observed a different phenomenon: the rock was observed to disk into a number of pieces at variable but higher confining pressures, closer to the compressive than tensile strength of the rock. Although they suspected that this may have occurred due to a jacket leak or intrusion of the jacketing material, they were able to find a number of cases where this did not seem to have occurred. In these cases there was no explosive discharge. Bridgman [3] also observed the same disking phenomena in jacketed specimens and similarly was inconclusive in his explanation of this phenomenon.

The Ring Paradox. In these experiments Bridgman snugly slipped a hard rubber ring over a steel rod and subjected them both to hydrostatic pressure. The ring was observed to fail with a single axial crack (Fig. 1b). The argument in this case was that all stresses and strains in the ring were compressive even though the failure was clearly of the tensile

type: hence the paradox. Since it seemed to us that the solution to these paradoxes (the ring and the jacketed pinching-off effect) may have some important applications in rock mechanics, we decided to repeat the ring experiments under several different conditions of applied load.

## Experimental Observations

We decided not to repeat the experiments with hard rubber because we could not determine the type Bridgman used, and because we wanted to avoid certain peculiarities of rubber such as viscoelasticity and the glassy transition that occurs at several hundred MPa and which is accompanied by a 10-14% volume reduction (Paterson, [4]). Instead we chose pyrex glass for the rings because of its extreme brittleness, its transparency (which would allow easy crack detection), and because it is obtainable with a very fine surface finish so that problems with stress concentrations at the rod-ring interface could be avoided as much as possible.

Technique. Pyrex glass tubes of nominal 16 mm internal diameter and 1.4 mm wall thickness were obtained that were tight sliding fits on polished and hardened steel rods. There was no measurable taper or ellipticity in either the rods or rings and the diametrical clearance was typically less than 2 μm. The tubes were cut to about 13 mm nominal lengths, their ends buffed, and fitted over the rods in the three configurations shown in Fig. 2: unjacketed, partially jacketed, and fully jacketed.

Strain gages, parallel and perpendicular to the axis of the rings, were attached in three approximately evenly spaced positions on the outer

surface of the rings. Strain gages were also attached to the ends of the rods to measure the compression of the steel. The linear compressibility of the steel and glass were measured as $.26 \times 10^{-2}$ and $1.13 \times 10^{-2}$ $GPa^{-1}$, respectively. The assembly was then placed in a fluid medium pressure vessel and the pressure was increased at a steady rate, usually 1 or 10 Mpa $min^{-1}$.

Case 1, Unjacketed. Stress-strain curves for both the axial and circumferential directions on the glass rings is shown in Fig. 3 for a typical experiment of this type. We show in the figure, for reference, the linear compressibility for both the steel and the pyrex.

On initial compression the circumferential strain of the ring is in accord with the pyrex compressibility. At a certain pressure, somewhat variable from experiment to experiment, contact occurred between the ring and rod and the circumferential strain in the ring stiffened up and followed the compressibility of the steel. At a higher pressure the ring suddenly snapped, and a strain-drop was observed on all three circumferential gages. This strain-drop was quite reproducible between experiments. When pressure was reduced, the ring followed the pyrex curve again. In each case the ring was found to have failed by a single throughgoing axial crack.

Case 2, Partially Jacketed. These experiments, illustrated in Fig. 4, were similar in many respects to those of Case 1. At low pressure, the ring compresses rapidly, as a hollow cylinder. At higher pressures its behavior is similar to that of Case 1, although failure typically occurred at a slightly higher total pressure. Fracture was again usually by a single throughgoing axial crack. In a few cases a horizontal crack formed; this was attributed to too much clearance between ring and rod,

so that loading prior to contact prestressed the ring in the circumferential direction and hence inhibited axial cracking. Notice the difference in the axial strains between Cases 1 and 2. In Case 1, since there was pressure fluid between the ring and rod, the axial strains followed the pyrex compressibility, indicating no frictional constraint between rod and ring. In Case 2, however, the axial strain of the ring was intermediate to that of pyrex and steel and exhibited hysteresis on unloading, indicating that the deformation of the ring was at least partially constrained by friction with the rod. This effect can also explain why the stress-drop in this case was not as abrupt as in case 1: it is partially restrained by friction until the fluid invades the ring-rod interface.

Case 3, Fully Jacketed. The behavior in the fully jacketed case was very different from that in the other two cases. Typical stress-strain curves are shown in Fig. 5. (Notice that the scales are much larger than in Figs. 3 or 4). After an initial compaction, the circumferential strain is strongly influenced by the steel, with no significant hysteresis. The axial strain is also affected by the steel, but not to the same extent as the circumferential one, and has considerable hysteresis on unloading. The ring, after testing, was usually observed to be cracked in an axial direction by a number of axial cracks, typically 2 to 6, which often extend the entire length of the ring but which almost never break the outer wall of the ring. One such crack is shown in Fig. 6.

No sudden strain drops or other unusual deviations were observed in the strain records. We conducted numerous experiments to different maximum pressure values in order to determine if there was a critical

pressure at which the cracks formed. We found that the cracks formed at anywhere between 200 and 700 MPa confining pressure, but in some cases the rings were found to have no visible cracks after being subjected to 700 MPa.

## Interpretation

The explanation for the unjacketed (Case 1) and partially jacketed (Case 2) observations is quite straightforward and follows the explanation of Jaeger and Cook [2] for the unjacketed case of the pinching-off effect.

In Case 1, after the ring is constrained by the rod, the hoop stress ($\sigma_\theta$) in the ring falls below the confining pressure (Pc). We calculated the difference ($\sigma_\theta$-Pc) at the inner wall of the ring and found this effective stress to be tensile, with a value of 30 $\pm$ 5 MPa at the time of rupture. This is close enough to the handbook value for the tensile strength of pyrex that we conclude that the ring failed by hydrofracturing, from the inside out in these experiments.

We did similar calculations for the partially jacketed case and obtained similar results. Thus in that case a tensile effective stress, approximately equal to the tensile strength of the glass, existed at the outer edge of the ring when failure occurred. Thus hydrofracturing again occurred, this time from the outside in.

The results for Case 3 are considerably more difficult to explain. In a number of aspects, case 3 resembles the disking observed by Jaeger and Cook [2] and Bridgman [3] for the jacketed pinching-off experiments.

Unlike Case 1 and 2, in Case 3 the cracks clearly formed stably. The evidence for this is: a) there were no offsets in the strain data; b)

multiple cracks formed; c) the cracks extended from the inner wall of the ring outwards, but did not reach the outer wall; and d) repeated experiments on the same specimen to successively higher pressures allowed us to observe crack growth (Fig. 6).

It is known that under overall compressive stresses, tension cracks can nucleate in brittle materials at preexisting flaws. This phenomenon has been illustrated by Brace and Bombolakis [5] and Hoek and Bieniawski [6] in glass plates containing preexisting straight cracks which make an acute angle with the direction of (uniaxial) compression. Similar experiments have been made by Nemat-Nasser and Horii [7] and Horii and Nemat-Nasser [8] using plates of Columbia resin CR39 which is brittle at room temperature. Figure 7 is a sketch of an experiment of this kind. Under increasing axial compression the upper face of the preexisting flaw PP' slides relative to the lower face, and, as a consequence, large tensile stresses develop at the crack tips P and P'. When the differential stress $|\sigma_1 - \sigma_2|$, attains a critical value, tension cracks nucleate at P and P', grow and curve toward the direction of the maximum compressive force. Nemat-Nasser and Horii [7, 8] show analytically and verify experimentally that crack growth of this kind is an inherently stable process if $\sigma_2$ is compressive, but that it becomes unstable after a critical crack length is obtained if $\sigma_2$ is tensile. These authors show that the cracks initiate at about 70° angle relative to the orientation of the initial flaw, for a wide variety of flaw orientations.

Scanning electron microscopy shows that the Case 3 fractures did initiate at surface flaws on the inside surface of the pyrex tubing. These fracture flaws were of complex geometry, generally having linear

dimensions of 10μm, or less; see Fig. 6. In the sequel, using simple estimates, we shall show that a flaw size of about 10μm is sufficient to nucleate tension cracks in pyrex glass under the overall compressive forces that seem to exist in Case 3. Once such a tension crack is nucleated, it will grow in a stable manner with increasing confining pressure.

Let $\sigma_z$, $\sigma_\theta$, and $\sigma_r$ be the axial, the hoop, and the radial stress, respectively. The elementary computations given in Appendix A show that all three stress components are compressive in the pyrex tubing, with $|\sigma_r| > |\sigma_z| > |\sigma_\theta|$ at its inner surface, and the magnitude of $\sigma_\theta$ increasing toward its outer surface. Therefore, if conditions for tension crack nucleation are right, then the crack will be nucleated at a preexisting surface flaw on the inside surface of the pyrex tubing, and will grow in the axial direction. On the other hand, if conditions are right for crack nucleation at an interior flaw of suitable geometry, then the tension crack will first grow toward the interior surface of the tubing and, hence, will become a surface flaw. Then this surface flaw may nucleate a tension crack which will curve and grow in the axial direction. In this case, the geometry of the initial surface flaw would be rather complex. In either case, the tension crack will have a sharp initial kink, will grow in the axial direction, and, since the magnitude of the hoop stress increases in the radial direction, the crack will never reach the outer surface of the pyrex glass, i.e., it will never become a through crack. Furthermore, its growth would be strictly a stable process. All these are borne out by scanning electron microscopic observations, as illustrated in Figs. 6A, B, C, and D.

To estimate the minimum size of a preexisting flaw which can produce tension cracks, we observe that: (1) because all principal stress components are compressive, the initial flaw will be closed and the Mode I stress intensity factor at its edges (prior to crack kinking) will be zero; and (2) locally at the edge of the preexisting flaw, the plane deformation conditions can be used to estimate the Mode I stress intensity factor associated with an initial out-of-plane crack nucleation.

Let $k_{II}$ be the Mode II stress intensity factor at the edge of a suitably oriented (three-dimensional) flaw (before any out-of-plane crack initiation); see Fig. 8. From the analysis of Hayashi and Nemat-Nasser [9] it follows that the opening mode stress intensity factor, $K_I$, at the tip of a small out-of-plane crack emanating from the flaw, can be estimated by

$$K_I = -(3/4)k_{II} (\sin \theta/2 + \sin 3\theta/2). \qquad (1)$$

The tension crack initiates in the direction $\theta$ which renders $K_I$ maximum at its tip. This direction is obtained by setting $\partial K_I/\partial\theta = 0$. It is about 70.5°.

For a general three-dimensional flaw, the value of $k_{II}$ depends on the geometry of the flaw and the far-field stresses in a rather complex manner [10]. A good estimate, however, can be obtained by considering an effective flaw length, 2c, and using a plane strain condition. This yields

$$k_{II} = (1/2) \quad \pi c (\sigma_1 - \sigma_2) \sin \gamma, \qquad (2)$$

where $\sigma_1$ is the maximum and $\sigma_2$ is the minimum compressive principal stress, and $\gamma$ is the orientation of the flaw measured from the $\sigma_1$-direction. $k_{II}$ is maximum when $\gamma = 45°$. Using this and $\theta = 70.5°$, we obtain from (1),

$$K_I = -0.577 \sqrt{\pi c}\,\sigma_1 (1 - \sigma_2/\sigma_1). \qquad (3)$$

For a three-dimensional flaw with a complex initial geometry, $K_I$ may be larger than the above estimate, but for our purposes, (3) seems quite adequate.

A tension crack initiates when $K_I$ attains its critical value $K_c$. Then, for given values of the stress components, Eq. (3) yields an estimate for the minimum flaw size necessary to nucleate a tension crack.

From the elementary analysis and data given in Appendix A, the stress ratio at the interior face of the pyrex glass tubing is estimated to be, $\sigma_\theta/\sigma_z = \sigma_2/\sigma_1 \approx 0.590$. Using the average value of $K_c \approx 0.5 MNm^{-3/2}$, for $\sigma_z = -300, -500, -700 MPa$, Eq. (3) yields $c = 16, 5, 3$ $\mu m$, respectively, which are of the right order of magnitude.

In the actual case, the complex geometry of a preexisting flaw can influence the value of $k_{II}$ and, therefore, the overall pressure at which a tension crack can be nucleated. Furthermore, the preexisting flaws are not flat and, therefore, once they nucleate tension cracks, the relative sliding of their surfaces produces local tension fields which drive these cracks in the direction of maximum compression, as applied overall pressure is increased. Such crack growth would be inherently a stable process.

The analysis presented above shows that under the state of stress associated with Case 3 experiments, tension cracks can nucleate from very small, preexisting flaws, and can grow in the axial direction. The analysis, however, does not explain why these tension cracks become as large as they do in the experiments. A plausible explanation is as follows.

In the elementary computations of Appendix A, the friction between the pyrex tubing and the steel bar has been neglected. In the experiment, on the other hand, the axial deformation of the pyrex tubing is somewhat constrained by the presence of this friction. Once tension cracks are nucleated, however, the frictional forces will be relaxed. This will have two effects: (1) it tends to increase the axial stress, $\sigma_z$, which actually drives the tension cracks in the axial direction, and (2) it tends to decrease the magnitude of the stress ratio, $\sigma_\theta/\sigma_z$, which, in turn, tends to increase the opening mode stress intensity factor, $K_I$, at the tip of the tension crack; see Eq. (3). Both of these tend to further drive the tension cracks in the axial direction, which, in turn, further relaxes the interfacial friction.

The experimental results for the axial strain in Fig. 5 seems to support this conjecture. As is seen, the initial slope of the loading portion in this figure, indicates a compressibility intermediate between steel and glass. The slope of the portion marked BC, however, is somewhat reduced, being quite close to the compressibility of the pyrex glass. This suggests that the axial constraint provided by the steel bar is somewhat diminished after point B. At point C the compressibility again changes abruptly. These irregular changes may indicate sticking and slipping in the friction between rod and ring as the cracks propagate.

## Discussion

The results for the jacketed case of the ring experiment, in which it was found that in a homogeneous brittle material axial mode I cracks would grow from initially small flaws for considerable distances in an all around compressive stress state, is instructive towards understanding several more conventional problems in rock mechanics.

In triaxial compression tests, dilatancy has been found to result from the growth of axial cracks, even at high confining pressure [11-13]. These studies have reached the conclusion that the shear crack mechanism of axial crack initiation [5-6] is unimportant because shear cracks are rarely observed in SEM studies. Furthermore, the type of analysis carried out previously [7-10] has been limited to cases where $\sigma_2$ is very low or tensile, so that even alternative crack initiation mechanisms [13] have not provided an explanation for the pervasive occurrence of long axial cracks under these experimental conditions. The experimental results and analysis presented here show, however, that axial cracks can be initiated by tiny flaws and grow stably for long distances under an overall compressive stress state. Thus shear cracks or other types of stress concentrations would not be necessarily expected to be prominent in SEM studies. In a heterogeneous material like rock, where stress concentrations such as those we observed at the ring-rod interface can be expected to commonly occur at grain boundaries, it is not surprising that axial cracking predominates.

Another application may be in blasting, where damage is produced by a radial shock wave propagating outwards from a cylindrical or spherical

cavity. In that case the stresses in the vicinity of the shock wave are usually all compressive, with the radial stress being much larger than the hoop stress, but radial tensile cracks are observed to propagate outwards behind the shock wave [14, 15]. The mechanism for the formation of such cracks may be similar to that discussed here, but dynamically driven by the shock loading.

## Acknowledgements

We thank Barry Raleigh and Keith Evans for critical reviews of the manuscript, S. Brown and S. Cox for helpful discussion, and Dee Breger for the SEM work. This work was supported by the Defense Advanced Research Projects Agency under contract F4960-84-C-0019. Lamont-Doherty Geological Observatory Contribution Number 0000.

## References


1. Bridgman, P.W., The Physics of High Pressure, Bell, London (1931).
2. Jaeger, J. C. and Cook, N.G.W., Pinching-off and disking of rocks, J. Geophys. Res., 68, 1759-65 (1963).
3. Bridgman, P.W., The Physics of Large Plastic Flow and Fracture, Harvard, Cambridge, Mass. (1964).
4. Paterson, M. S., Effect of pressure on Youngs' modulus and the glass transition in rubber, J. Appl. Phys., 35, 176-179 (1964).
5. Brace, W. F. and Bombolakis, E.G., A note on brittle crack growth in compression, J. Geophys. Res., 68, 3709-3713 (1963).
6. Hoek, E. and Bienawski, Z.T., Brittle fracture propagation in rock under compression, Int. J. Fract. Mech., 1, 137-155 (1965).
7. Nemat-Nasser, S. and Horii, H., Compression-induced nonplanar crack extension with application to splitting, exfoliation, and rockburst, J. Geophys. Res., 87, 6805-6821 (1982).
8. Horii, H. and Nemat-Nasser, S., Compression induced microcrack growth in brittle solids: Axial splitting and shear failure, J. Geophys. Res., 90, 3105-3125 (1985).
9. Hayashi, K. and Nemat-Nasser, S., Energy release rate and crack kinking, Int. J. Solid Struct., 17, 107-114 (1981).
10. Murakami, Y. and Nemat-Nasser, S., Growth and stability of interacting surface flaws of arbitrary shape, Eng. Fract. Mech., 17, 193-210 (1983).
11. Tapponnier, P. and Brace, W. F., Development of stress-induced microcracks in Westerly granite, Int. J. Rock Mech. Min. Sci., 13, 103-112 (1976).

12. Kranz, R.L., Crack growth and development during creep of Barre granite, Int. J. Rock Mech. Min. Sci., 16, 23-35 (1979).

13. Holcomb, D.J. and Stevens, J., The reversible Griffith crack: A viable model for dilatancy, J. Geophys. Res., 85, 7101-7107 (1980).

14. Rinehart, J.S., Dynamic fracture strengths of rocks, Proc. Seventh Symp. Rock Mech., Penn. State Univ., 117 (1965).

15. Grady, D.E. and Kipp, M.E., The micromechanisms of impact fracturing of rock, Int. J. Rock Mech. Min. Sci., 16, 293-302 (1979).

## Figure Captions

Fig. 1. A schematic diagram of the two paradoxical experiments of Bridgman. A) The pinching-off effect; B) the ring paradox.

Fig. 2. Schematic diagrams of the three experimental configurations. A) Unjacketed; B) partially jacketed; and C) jacketed.

Fig. 3. Stress-strain curves for the ring in an unjacketed case: a) circumferential strain; b) axial strain. Linear compressibility curves for the glass and steel are shown for reference.

Fig. 4. Stress-strain curves for the ring in a partially jacketed case.

Fig. 5. Stress-strain curves in a jacketed case. See text for discussion of points B and C on axial stress-strain curve.

Fig. 6. SEM photomicrographs of an axial crack formed in a jacketed experiment, shown at successively greater magnifications A, B, C, D. This was a cycled experiment, and several successive positions of the crack front can be seen. The view is perpendicular to the fracture plane, with the inside surface of the pyrex ring appearing at the bottom of each photograph. The crack starts at a complex flaw at the center, and an abrupt jog in the crack plane extends from the flaw. Arrest lines from repeated pressurizations are visible in (A) and (B).

Fig. 7. Sketch of the growth of tensile cracks from a sliding crack. Opposing surfaces at the initial flaw PP' slide due to differential stress, producing tension cracks PQ and P'Q'.

## Appendix A

To estimate the state of stress in the pyrex tubing, we assume linearly elastic deformation, denote Young's modulus and Posson's ratio of the glass by E and $\nu$, and those of steel by $E_s$ and $\nu_s$, respectively. Ignoring the frictional forces between the glass tubing and the steel, the radial displacement of the steel may be estimated by

$$u_s = \frac{1}{E_s} [\nu_s p_o - (1-\nu_s) p_i] \, r, \tag{A.1}$$

where $p_o$ is the applied overall confining pressure, $p_i$ is the pressure transmitted across the glass-steel interface, and $r$ measures length in the radial direction. In the absence of friction, the state of stress in the tubing is given by

$$\sigma_z = -p_o,$$

$$\sigma_\theta = \frac{a^2 p_i - b^2 p_o}{b^2 - a^2} + \frac{(p_i - p_o) a^2 b^2}{r^2 (b^2 - a^2)},$$

$$\sigma_r = \frac{a^2 p_i - b^2 p_o}{b^2 - a^2} - \frac{(p_i - p_o) a^2 b^2}{r^2 (b^2 - a^2)} \tag{A.2}$$

and the corresponding radial displacement is

$$u_g = \left[\frac{1-\nu}{E}\,\frac{a^2p_i-b^2p_o}{b^2-a^2} + \nu\frac{p_o}{E}\right] r +$$

$$\left[\frac{1+\nu}{E}\,\frac{(p_i-p_o)\,a^2b^2}{b^2-a^2}\,\frac{1}{r}\right] \qquad (A.3)$$

where a is the inside and b the outside radius of the tubing. At the glass-steel interface the radial displacements must match, which yields an equation for $p_i$ in terms of $p_o$, as follows:

$$\frac{p_i}{p_o} = [2+(k_o\nu_s-\nu)\,(1-\beta^2)]/[(1-\nu)\beta^2+(1+\nu)+k_o(1-\nu_s)(1-\beta^2)],$$

$$k_o = E/E_s, \qquad \beta = a/b. \qquad (A.4)$$

In the experiments, $E = 5.6 \times 10^4$ MPa, $E_s = 2.1 \times 10^5$ MPa, $\nu = 0.21$, and $\nu_s = 0.23$. For tubing with 15.9 mm internal and 18.6 mm external radius, we obtain $p_i = 1.064p_o$. Then, $\sigma_\theta/p_o = -0.59$.

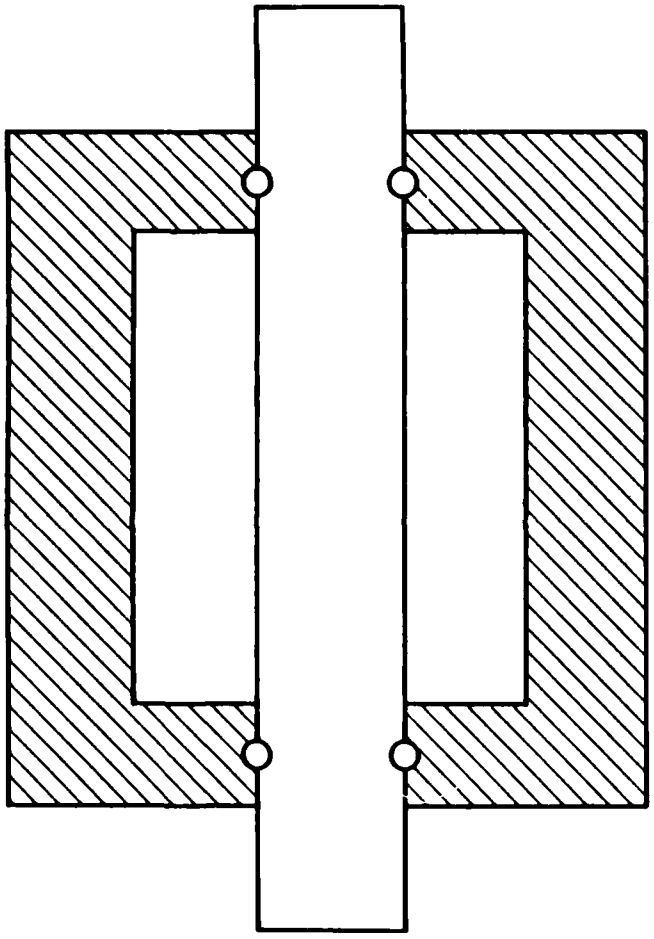

a.

PINCHING–OFF EFFECT

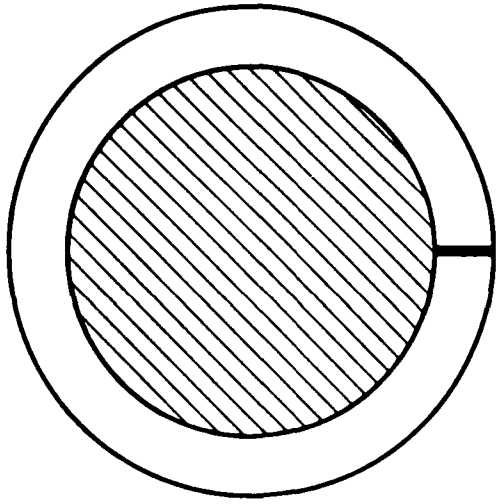

b.

RING PARADOX

FIG 1

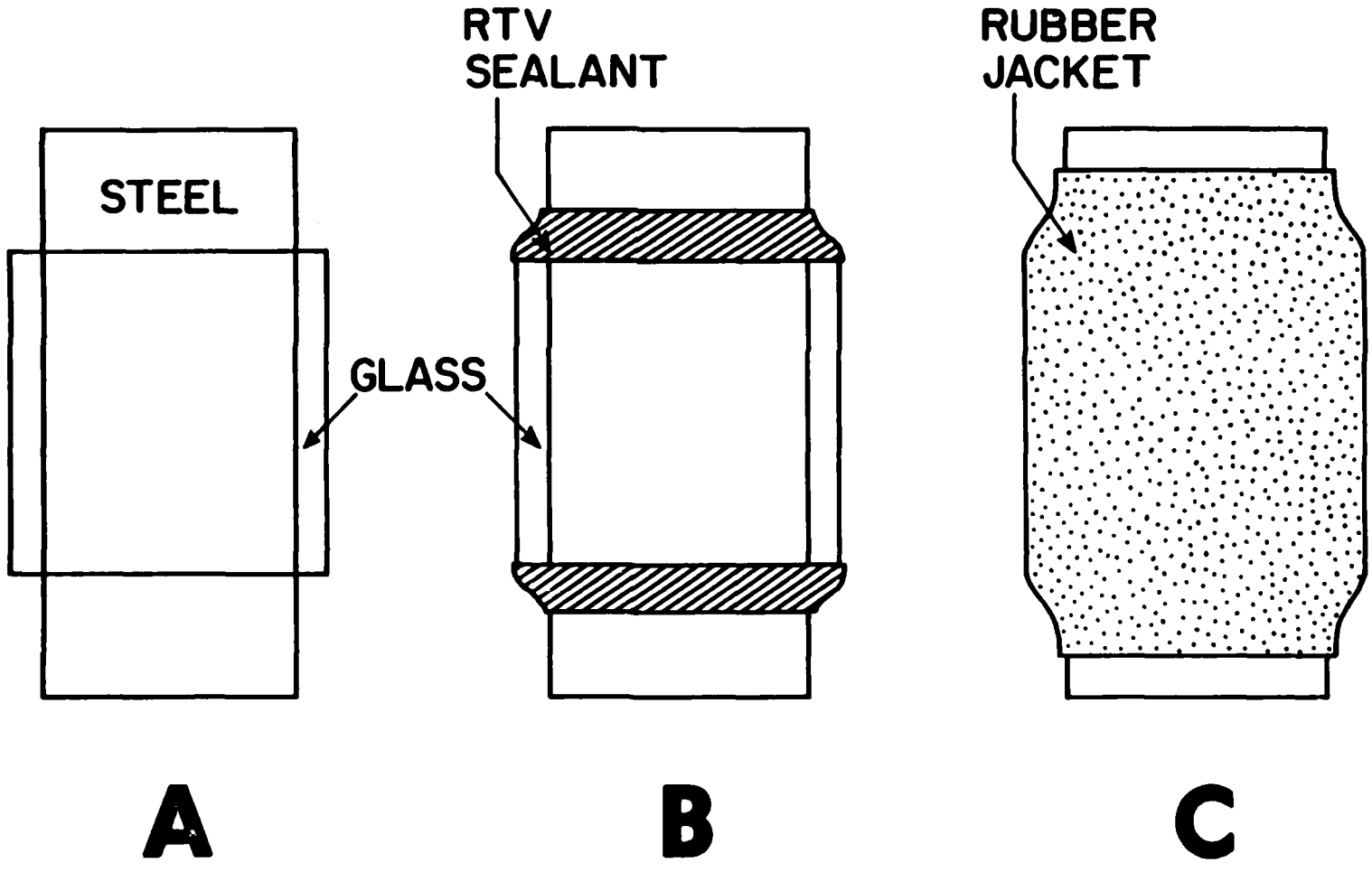
STEEL
GLASS
RTV
SEALANT
RUBBER
JACKET
A
B
C

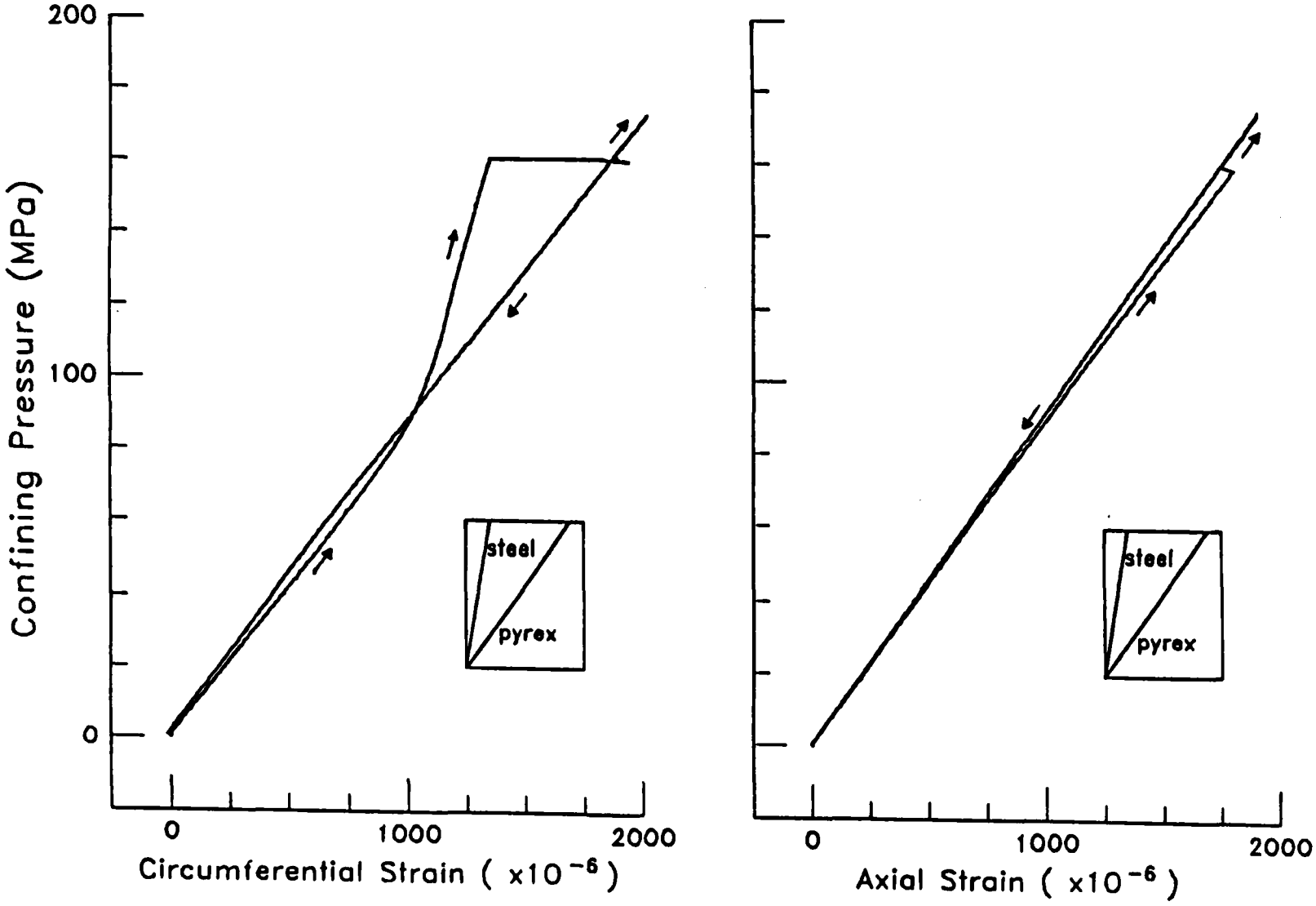
200
100
0
Confining Pressure (MPa)
steel
pyrex
0
1000
2000
Circumferential Strain ( x10 -6 )
steel
pyrex
0
1000
2000
Axial Strain ( x10 -6 )

FIG 3

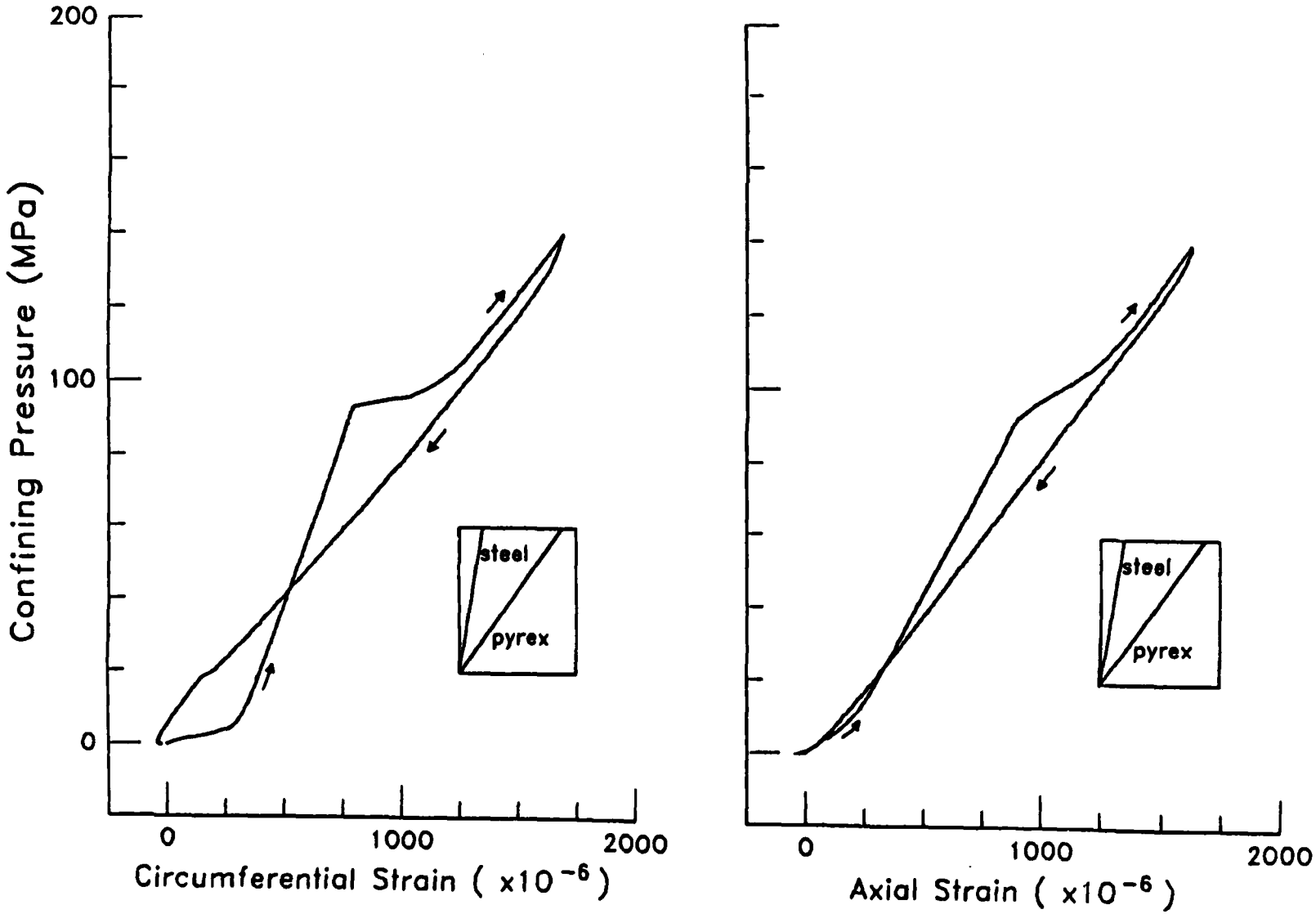
200
100
0
Confining Pressure (MPa)
steel
pyrex
0
1000
2000
Circumferential Strain ( x10 -6 )
steel
pyrex
0
1000
2000
Axial Strain ( x10 -6 )

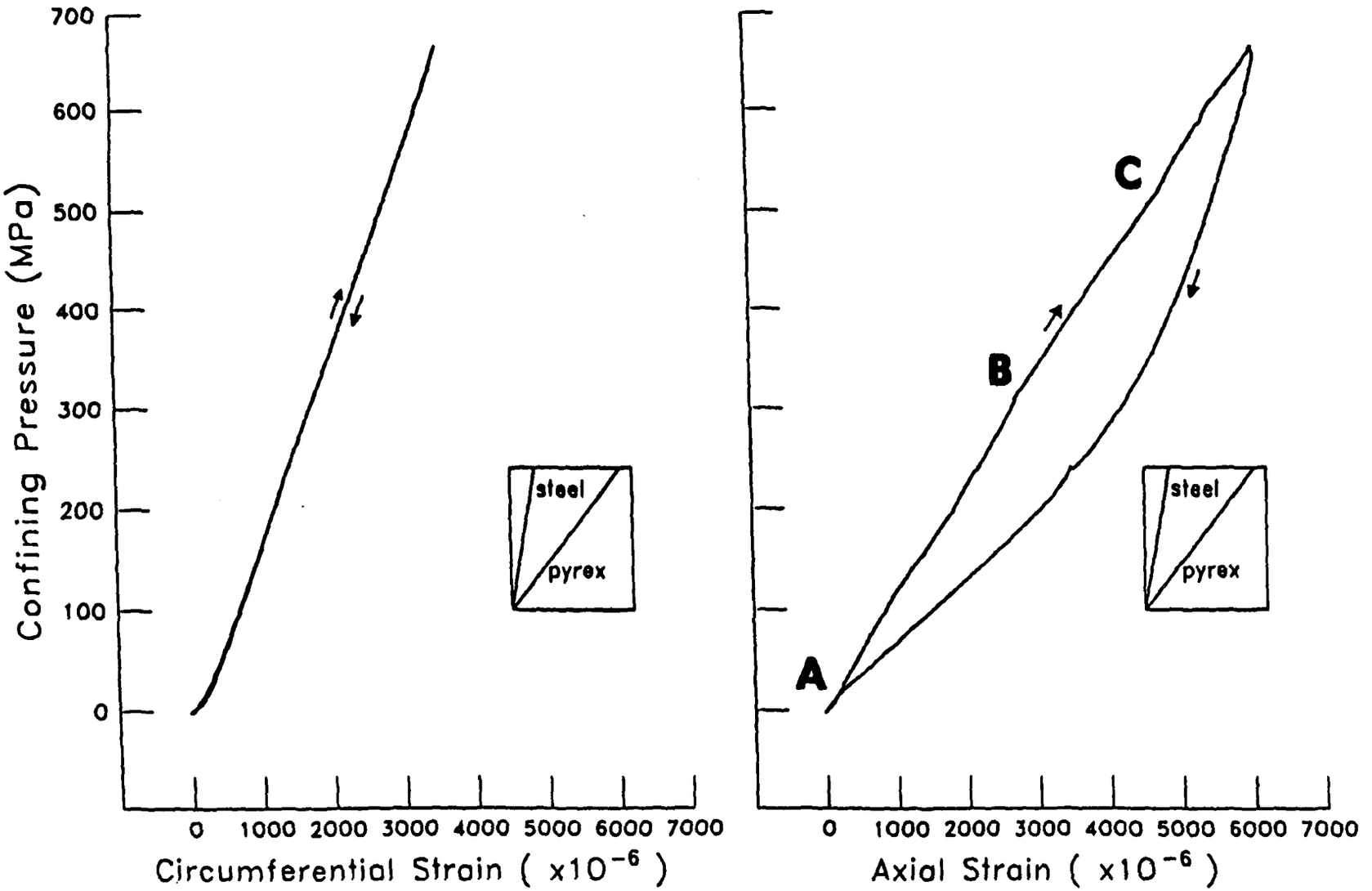
Confining Pressure (MPa)
700
600
500
400
300
200
100
0
0 1000 2000 3000 4000 5000 6000 7000
Circumferential Strain ( x10⁻⁶ )
steel
pyrex
A
B
C
0 1000 2000 3000 4000 5000 6000 7000
Axial Strain ( x10⁻⁶ )
steel
pyrex

Fig 5

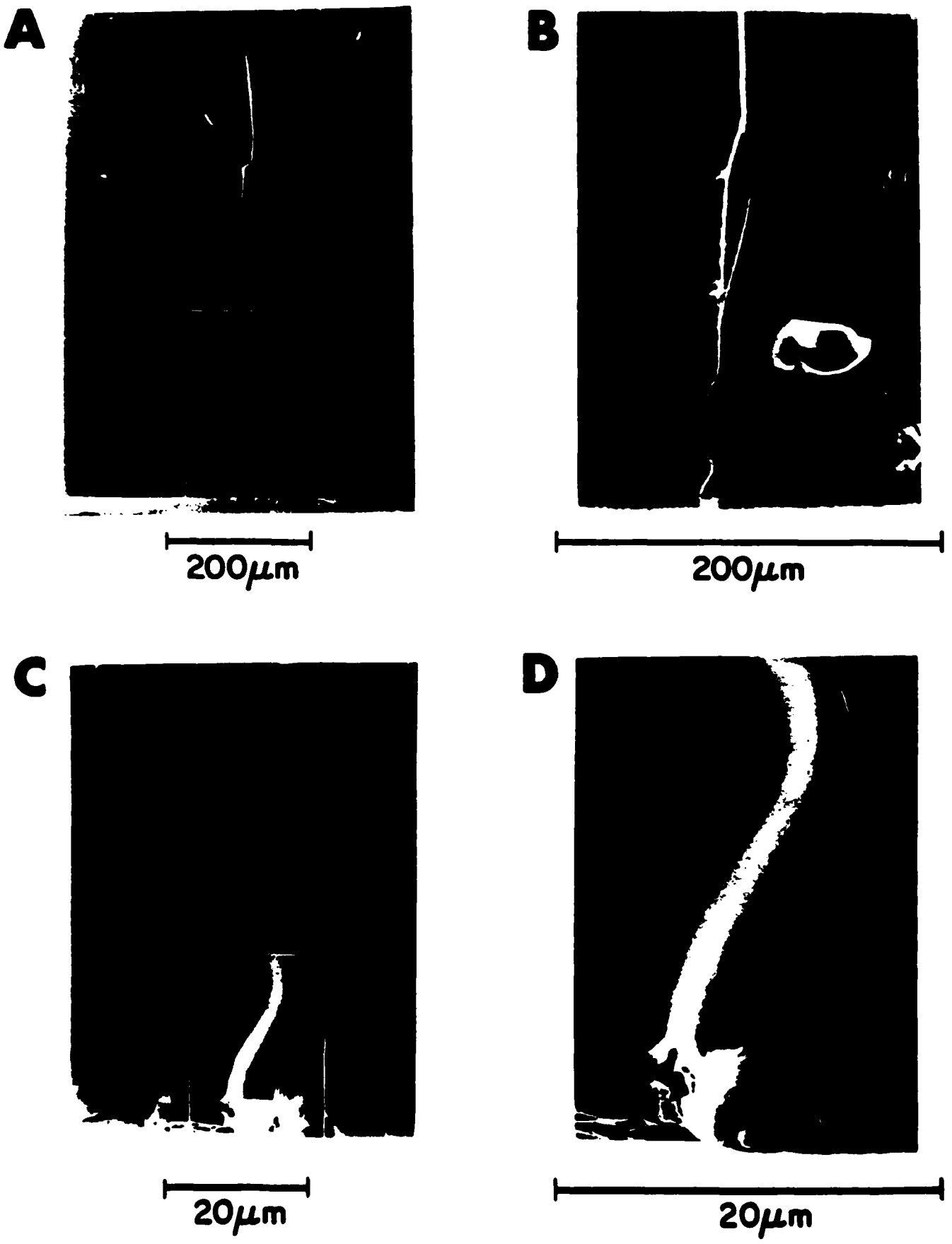


Fig. 6.

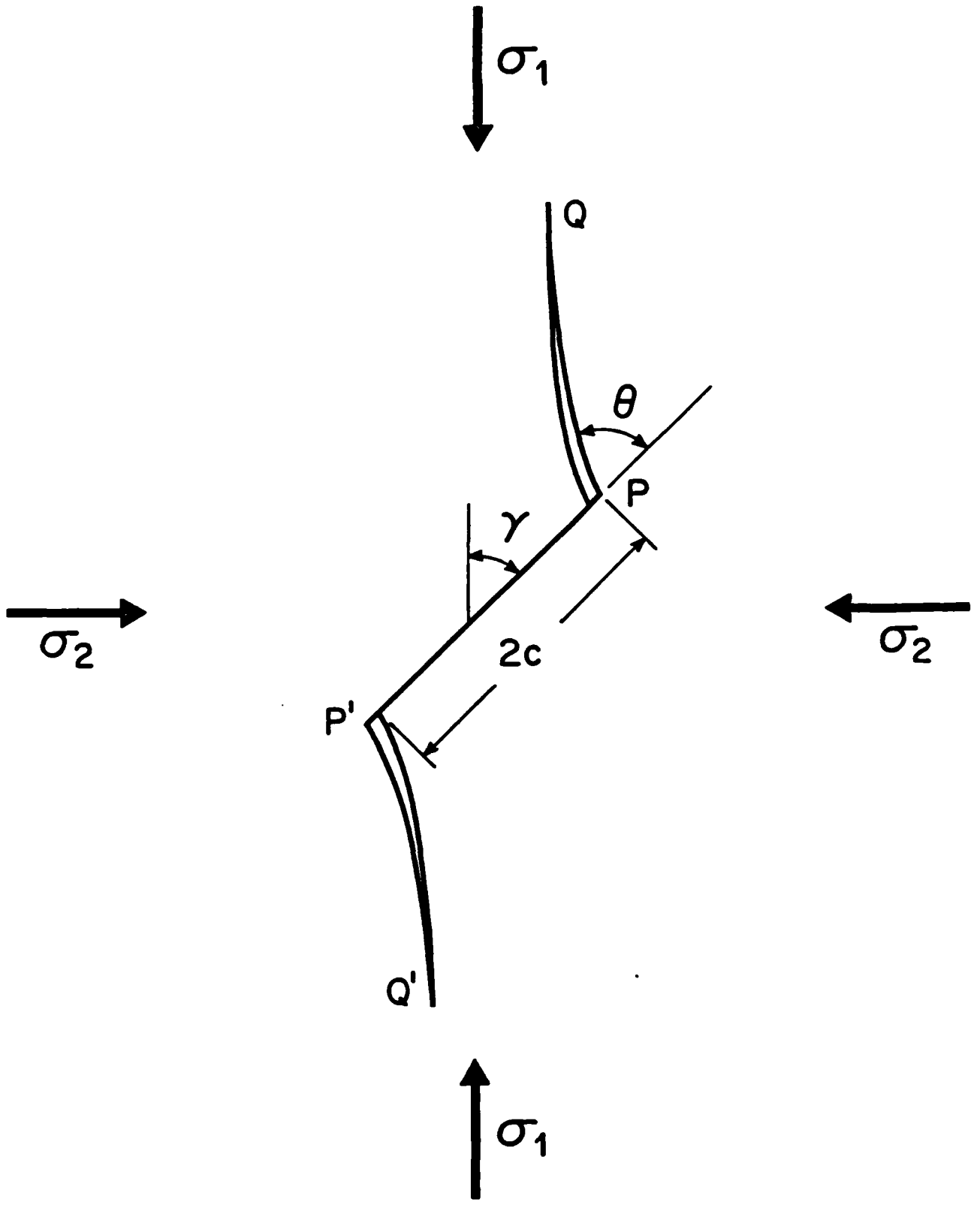


FIG 7